Desalination and Water Treatment
www.deswater.com
doi: 10.1080/19443994.2015.1035495

57 (2016) 9148–9165
April

Taylor & Francis
Taylor & Francis Group

CCD series no-13: illustrating low-energy SWRO-CCD of 60% recovery and BWRO-CCD of 92% recovery with single element modules without energy recovery means—a theoretical extreme case study

Avi Efraty

Desalitech Ltd, P.O. Box 132, Har Adar 90836, Israel, email: avi@desalitech.com

Received 11 October 2013; Accepted 3 March 2015

ABSTRACT

In contrast with the conventional SWRO and BWRO plug flow desalination (PFD) techniques where recovery depends on the number of lined membrane elements and energy consumption on the efficiency of energy recovery device (ERD), the newly conceived closed-circuit desalination (CCD) technologies enable the attainment of high recovery, irrespective of the number of elements per module with low energy consumption without need for ERD. The present theoretical model analysis describes the extreme performance prospects of CCD illustrated by a single-element SWRO–CCD unit performing up to 60% recovery with near absolute energy efficiency without need for ERD (e.g. 50% recovery; 13 lmh; 1.573 kWh/m^3 for 32,000 ppm NaCl feed equivalent to ocean seawater of 35,000 ppm) as well as by a single-element BWRO–CCD unit performing up to 92% recovery with low energy (e.g. 90% recovery; 25 lmh; 0.472 kWh/m^3 for 1,500 ppm NaCl feed equivalent to common brackish water sources of 1,700–2,000 ppm). Another illustration pertains to the performance of a single-element BWRO–CCD–PFD unit, wherein replacement of brine by fresh feed takes place at the end of each CCD sequence by a brief PFD step with results showing only a minor increase in energy consumption compared with that of BWRO–CCD (e.g. 90% recovery; 25 lmh; 0.488 kWh/m^3 for 1,500 ppm NaCl feed). The illustrated theoretical model's results show good agreement with experimental data and manifest the conceptual differences between CCD and conventional RO techniques at their extreme.

Keywords: CCD; SWRO; BWRO; Compact RO units; High recovery; Low energy; Solar panels energy; Wind turbines power

1. Introduction

Increased recovery as the function of the length of lined elements and the need to recover energy from the pressurized brine effluent to achieve high energy efficiency are the basic principles of conventional SWRO and BWRO plug flow desalination (PFD) techniques since inception some 55 years ago by Loeb and Sourirajan [1], although the major components (e.g. membranes, pumps, ER devices, etc.) used today in the so-called conventional techniques are modern and enable a near state-of-the-art performance within the technological limitations. Depletion and deterioration of global fresh water sources, viewed in the context of growing demand for fresh water supplies due to the rapidly expanding global population, increased the standards of living and rising energy costs have created urgent needs for improved RO technologies.

Short- and long-term future projections [2,3] reveal increased reliance on RO for fresh water supplies worldwide and the needs to increase recovery and reduce energy consumption by advanced RO techniques. Since conventional RO techniques are already practiced at their near state-of-the-art level with very little room for further improvements, it has become obvious that new advanced technologies need to be developed in order to meet future goals and targets for water treatment and desalination.

Seawater of 3–5% salinity constitutes ~99% of the water on earth with only ~1.0% of the total representing recycled fresh water through rains and melting of snow and ice with small amounts also found in the form of renewable brackish water sources. The aforementioned imply the increasing future role of SWRO desalination for fresh water supplies and supplements and this trend has began already in various parts of the world along seawater shores in response to fresh water shortages. The emphasis on SWRO in future projections is important especially with regards to energy consumption, which is the major contributor to current seawater desalination costs.

In order to meet future targets [2,3], newly conceived advanced RO technologies will most obviously need to depart from the principles of conventional RO PFD methods, which are already practiced at their near state-of-the-art level. In this context noteworthy are the recently reported [4–13] closed-circuit desalination (CCD) technologies which exemplify how future goals and targets can be met already today by a new approach to RO on the basis of entirely different operational principles compared with those of conventional RO. Common knowledge of conventional RO systems covered in manuals of all membranes producers (e.g. Filmtec Manual [14]) and their computer design programs implies the need for designs such as that in Fig. 1 with modules comprising 7–8 elements each and effective energy recovery device (ERD) means in order to effect SWRO desalination of 45–50% recovery with reasonable energy consumption. Likewise, the design of conventional BWRO desalination systems requires staged vessels of 4–6 elements each with lines of 12 and 18 elements inside to effect 75–85% and 85–90% recovery, respectively, with turbocharger means to save on energy. Conventional PFD designs leave no doubt that recovery is a function of the number of lined elements with energy consumption depending on flux, recovery, and ERD means. After 55 years of widespread practice and extensive experience with conventional PFD techniques, viewing a technology such as CCD of near absolute energy efficiency without the need of ERD means with recovery independent on the number of elements in modules creates a notion of untrustworthy magic even by well-experienced skilled engineers in the area of RO applications. Obviously, CCD is not magic since it complies with all the principles of RO including the basic equations of water flux and reverse salt flux with their respective permeability and salt diffusion coefficients, although the operational principles of CCD and PDF techniques are entirely different. The origin of the SWRO–CCD and BWRO–CCD technologies [4–13] is from theoretical model simulations; by now, more than 40 such units were installed in Israel and elsewhere and the experience gained with their operation over the past four years reveals consistent and reliable performance of high recovery, irrespective of the number of elements in modules, of low energy consumption with reduced fouling characteristics.

The present work describes theoretical extreme case studies of low-energy SWRO–CCD of 60% recovery and BWRO–CCD of 92% recovery with single element module apparatus without ERD means, supported by experimental results under conditions inconceivable in terms of conventional RO techniques, and thereby illustrating the validity of the new CCD approach to RO desalination.

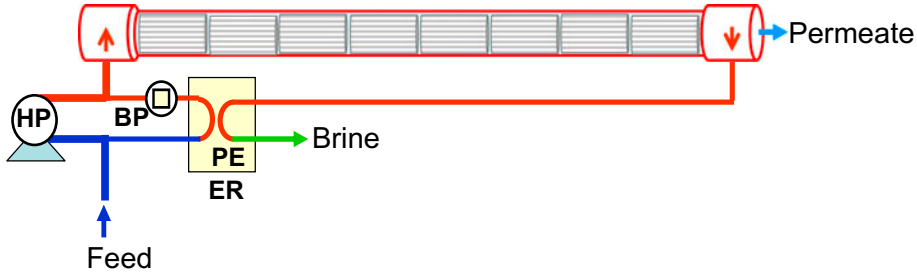

Fig. 1. Conventional SWRO unit comprising a single module of 8 element in line with its high pressure pump (HP), pressure exchanger for energy recovery (PE-ER), and booster pump (BP).

2. Illustration of high-recovery of low-energy SWRO–CCD with a single element unit without need for ERD

The schematic design of a SWRO–CCD unit with a single element module displayed in Fig. 2 comprises a single pressure vessel (8´´) with SWC6-MAX element (8´´) inside, high pressure pump with *vfd* (HP–*vdf*), circulation pump with *vdf* (CP–*vdf*), actuated valve (AV) and check valve (OWV—one-way valve) means, side conduit (SC) made of a pressure vessel with the same intrinsic volume of the closed circuit, and conduit lines for pressurized and none pressurized flow in various section of the apparatus. The unit is operated with fixed flow rates of HP and CP under variable pressure conditions in consecutive sequential batch modes and when the desired batch recovery is attained at a distinct applied pressure, brine in the closed circuit is replaced by fresh feed through engagement with the pressurized SC, while desalination is continued nonstop. After all the brine in the closed circuit is replaced by fresh feed, the SC conduit is disengaged from the closed circuit, decompressed, its brine content replaced by fresh feed at near atmospheric pressure, then sealed, compressed and left on stand-by for the next engagement with the closed circuit. Compression and decompression of the SC take place under hydrostatic conditions with negligible energy losses and for this reason the process under review proceeds with near absolute energy efficiency.

The CCD simulated model performance at 25°C, 13 lmh, and 10% element recovery of the unit under review with 3.2% NaCl, equivalent to typical ocean water of 3.5%, is illustrated in Table 1 for the SWC6-MAX [15] element, assuming 85% efficiency of HP, typical of the DANFOSS pump, and 75% efficiency of the CP pump. The columns in Table 1, labeled at the bottom A1 → A17, stand for the followings: A1 for the mode of operation; A2 for the number of cycles in the batch sequence, A3 for the module inlet concentration; A4 for the module outlet concentration; A5 for the elapsed sequence time; A6 for the applied pressure; A7 for the average applied pressure; A8 for HP power; A9 for CP power; A10 for the combined HP + CP power; A11 for specific energy at a cited cycle; A12 for the combined permeate volume at a cited cycle; A13 for the average combined power at a cited cycle; A14 for the average specific energy at a cited cycle; A15 for batch recovery at a cited cycle; A16 for the permeate TDS at a cited cycle; and A17 for the average permeate TDS at a cited cycle. The principle data in Table 1 were generated as follows: applied pressure by Eq. (1); HP power by Eq. (2); CP power by Eq. (3); batch sequence recovery by Eq. (4); and permeate TDS by Eq. (5) with *pf* expressed by Eq. (6). The calculated pf according to Eq. (6) with $k = 0.45$ gave the best agreement with IMS design data and Δp was calculated using Eq. (7).

$$p_{\text{appl}} = \mu/A/T_{\text{CF}} + \Delta\pi_{\text{av}} + \Delta p/2 + p_{\text{p}} - \pi_{\text{p}} \tag{1}$$

$$P(\text{HP}) = Q_{\text{f}} \times p_{\text{appl}}/36/f_{\text{HP}} = Q_{\text{p}} \times p_{\text{appl}}/36/f_{\text{HP}} \tag{2}$$

$$P(\text{CP}) = Q_{\text{CP}} \times \Delta p/36/f_{\text{CP}} \tag{3}$$

$$\text{Batch Sequential Recovery} = \Sigma V_{\text{p}}/\left(\Sigma V_{\text{p}} + V\right) \times 100 \tag{4}$$

$$C_{\text{p}} = B \times C_{\text{f}} \times pf \times T_{\text{CF}}/\mu \tag{5}$$

$$pf = 10^{(k \times Y)} \tag{6}$$

$$\Delta p = (8/1{,}000) \times n \times [(Q_{\text{mi}} + Q_{\text{mo}})/2\times]^{1.7} \tag{7}$$

The parameters of Eqs. (1)–(7) are as followed: μ is flux (lmh); A—permeability coefficient (l/m^2/h/bar);

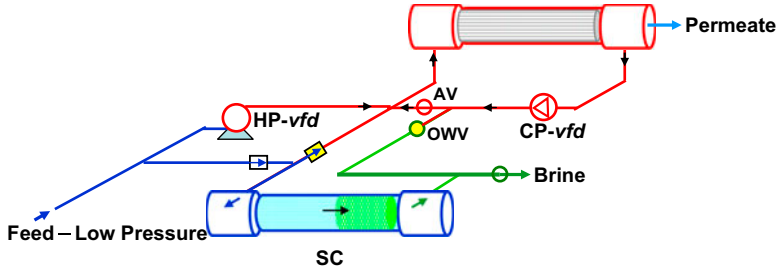

Fig. 2. A CCD unit for continuous consecutive sequential batch operation comprising a single module with a single element (8´´), high pressure pump with *vfd* (HP–*vfd*), circulation pump with *vfd* (CP–*vfd*), SC, and AV and check valve (OWV—one-way valve) means to enable engagement/disengagement of the SC with the closed circuit of the unit.

T_{CF}—temperature correction factor; $\Delta\pi_{av}$—average module concentrate-side osmotic pressure (bar); Δp—pressure difference (bar) of CP; p_p—permeate release pressure (bar); π_p—module permeate-side osmotic pressure (bar); P—power (kW); Q_f—pressurized feed flow rate (m^3/h); Q_p—permeate flow rate (m^3/h); ΣV_p—combined permeates volume (m^3) at a cited cycle; V—intrinsic free volume (m^3) of closed circuit; f—efficiency ratio of cited pump; C_p—concentration of permeates; C_f—concentration of feed; B—salt diffusion coefficient ($l/m^2/h$); Y—element recovery (10%); $n = 1$—a single element module, Q_{mi} ($=Q_p + Q_{CP}$)—module inlet flow rate; and Q_{mo} ($=Q_{CP}$)—module outlet flow rate.

The simulation in Table 1 reveals the need for a consecutive batch sequence duration of 4.77 min with 14 CCD cycles in the variable pressure range 35.9 → 72.2 bar to enable the production of 0.52 m^3/h permeate of 445 average ppm TDS with 60.9% recovery and average specific energy of 1.802 kWh/m^3. The maximum pressure of 72.2 bar is an operational set point which initiates the engagement of the SC to the closed circuit for replacement of brine by fresh feed, and thereafter the pressure drops to its minimum level (35.9 bar). If the maximum selected pressure of operation is restricted to 58.2 bar, the system will perform 50% recovery with a batch sequence duration of 3.07 min of 9 CCD cycles in the variable pressure range 35.9 → 58.2 bar and produce 0.52 m^3/h permeate of 377 ppm average TDS with an average specific energy of 1.573 kWh/m^3. Sequential batch variations of pressure, specific energy, and permeate TDS during the single element SWRO–CCD of 3.2% NaCl with up to 60.9% recovery according to the data in Table 1 are displayed in Fig. 3(A)–(C).

3. Illustration of high-recovery low-energy BWRO–CCD with a single element unit without need for ERD

The application of CCD for brackish water desalination is illustrated in Table 2 with the theoretical model performance simulation of the BWRO–CCD single element (ESPA2-MAX) [16] unit of the design displayed in Fig. 2 at 25˚C, 25 lmh, and 15% element recovery with feed of 1,500 ppm NaCl, representative of common brackish water sources of 1,700—2,000 ppm TDS depending on specific compositions. The theoretical model analysis data in Table 2 were generated by the same equations already cited in the context of Table 1. The sequential performance simulation data in Table 2 of 92% maximum recovery comprise 65 CCD cycles which are represented in the table by the following sections: 10 → 7 cycles (0 → 55.3% recovery), 47 → 52 cycles (89.2 → 90.2% recovery), and 60 → 65 cycles (91.4 → 92.0% recovery). Variations encountered in the consecutive sequential BWRO–CCD process according to the model analysis under review are displayed in Fig. 4(A)–(C) and pertain to applied pressure (A), specific energy (B), and permeate TDS (C). The maximum applied pressure set point selection in the model analysis under review determines the sequence period duration, recovery, permeate TDS, and energy consumption as exemplified next from the stand point of recovery. The attainment of 80.2 → 85.0 → 87.6 → 90.0 → 92.0% recovery in the model under review corresponds to the respective maximum sequential pressure set point selections of 11.0 → 12.9 → 14.5 → 16.8 → 19.7 bar, which effects the respective changes (in parenthesis) of sequence period duration (6.5 → 9.0 → 11.3 → 14.3 → 18.3 min), permeate average TDS (27 → 33 → 39 → 48 → 58 ppm), and specific energy (0.355 → 0.390 → 0.420 → 0.462 → 0.516 kWh/m^3). Energy requirements in RO also depend on the efficiency of pumps and in this context the selected efficiency ratio of 0.75 was assigned to the pumps cited in Table 2.

4. Illustration of high-recovery low-energy BWRO–CCD–PFD with a single element unit without need for ERD

High-recovery CCD of brackish water of low energy can be carried out effectively and efficiently also without need of SC using the simple unit design displayed in Fig. 5(A)–(B) with a single module single element configuration—the configuration may include any desired number of elements and the focus of a single element design is made only in the context of the current study. The design in Fig. 5 is of a typical batch CCD with valve means to enable the replacement of brine by fresh feed before a new batch is initiated. Making this process continuous is enabled by the replacement brine with fresh feed under PFD conditions by the two actuation modes (CCD and PFD) of the unit as specified in Fig. 5. The theoretical model performance simulation of the single element (ESPA2 MAX) [16] BWRO–CCD–PFD unit of the design displayed in Fig. 5 with 1,500 ppm NaCl feed under CCD conditions of 25˚C, 25 lmh, and 15% element recovery and PFD conditions of 25˚C, 4.7 lmh, 15% element recovery, and feed flow greater by 25% compared with that of the former mode is revealed in Table 3 for recovery up to 92.0%. Consecutive sequential variations during the BWRO–CCD–PFD operation under review are illustrated in Fig. 6(A)–(C) in

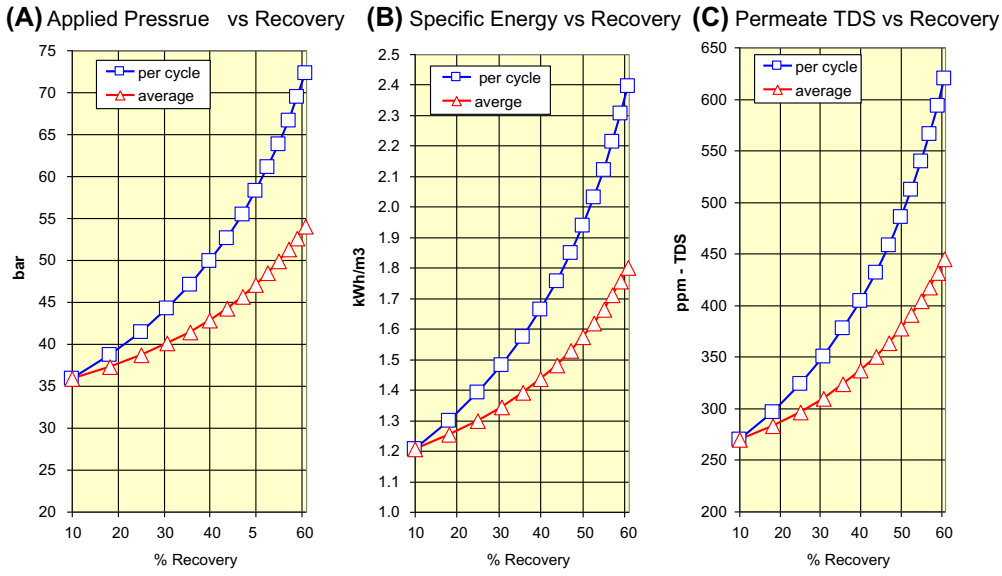

Fig. 3. Sequential batch variations of pressure (A), specific energy (B), and permeate TDS (C) during SWRO–CCD of 3.2% NaCl with up to 60.9% recovery according to the data in Table 1 with the single element (SWC6-MAX) apparatus of the design displayed in Fig. 2.

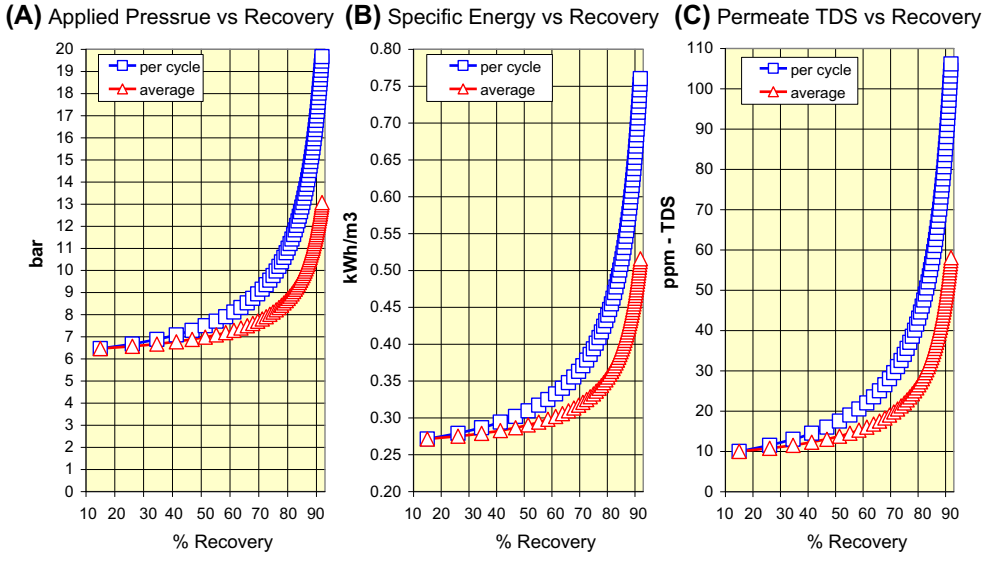

Fig. 4. Sequential batch variations of pressure (A), specific energy (B), and permeate TDS (C) during BWRO–CCD of 1,500 ppm NaCl with up to 92% recovery according to the data in Table 2 with the single element (ESPA2 MAX) apparatus of the design displayed in Fig. 2.

reference to the applied pressure (A), specific energy (B), and permeate TDS (C).

The performance differences between BWRO–CCD (Table 2—Fig. 4) and BWRO–CCD–PFD (Table 3—Fig. 6) with the same feed (1,500 ppm NaCl) are evident from the respective figures of the same parameters and manifest the effects of the brief PFD step of brine replacement by fresh feed in the latter. In

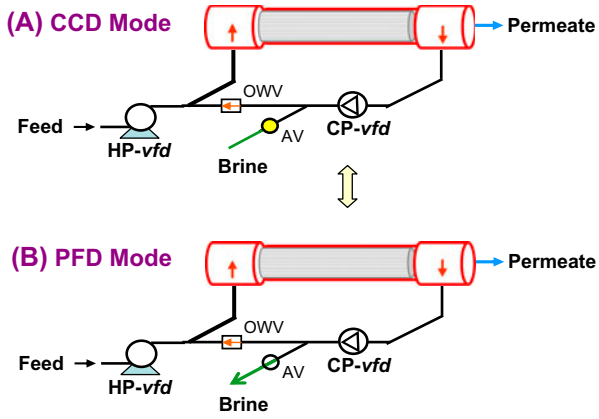

Fig. 5. A CCD unit for batch or for continuous consecutive sequential batch operation comprising a single module with a single element (8´), high pressure pump with *vfd* (HP–*vfd*), circulation pump with *vfd* (CP–*vfd*), and AV and check valve (OWV—one-way valve) means and its principle actuation modes of CCD and PFD.

the analysis under review in Table 3, the operation of CP is stopped during PFD, feed flow raised by 25% compared with CCD (1.02 → 1.28 m^3/h), and pressure is dropped to 2.4 bar. During the PFD step in the process, the flux is reduced to 4.7 lmh with average element recovery of 15% and the complete replacement of brine by fresh feed takes 1.5 min and proceeds with a relatively high energy (0.586 kWh/m^3) with poor permeates production (58 ppm TDS) as result of the low operational flux. The intent of the low-pressure low-flux PFD operation during the PFD step is to minimize the loss of energy at an expense of increased TDS of permeates. PFD in front of CCD does effect the increased feed concentration at the start of the latter (0.15 → 0.18%) as function of the recovery in of the former. Since the PFD step is brief, its overall effects on the performance decline with increased sequence period of increased sequence recovery. The differences between BWRO–CCD and BWRO–CCD–PFD (in brackets) are manifested at the recovery levels 80.2 → 85.0 → 87.6 → 90.0 → 92.0% by the respective maximum applied pressure of 11.0(11.4) → 12.9(13.2) → 14.5(14.7) → 16.8(16.9) → 19.7(19.6)bar, average permeate TDS of 27(31) → 33(38) → 39(44) → 48(53) → 58(64)ppm, and average specific energy of 0.355 (0.393) → 0.390(0.422) → 0.420(0.450) → 0.462(0.488) → 0.526(0.538) kWh/m^3. The aforementioned differences on the 80 → 92% recovery scale translate to the respective changes of 15 → 10% in TDS and

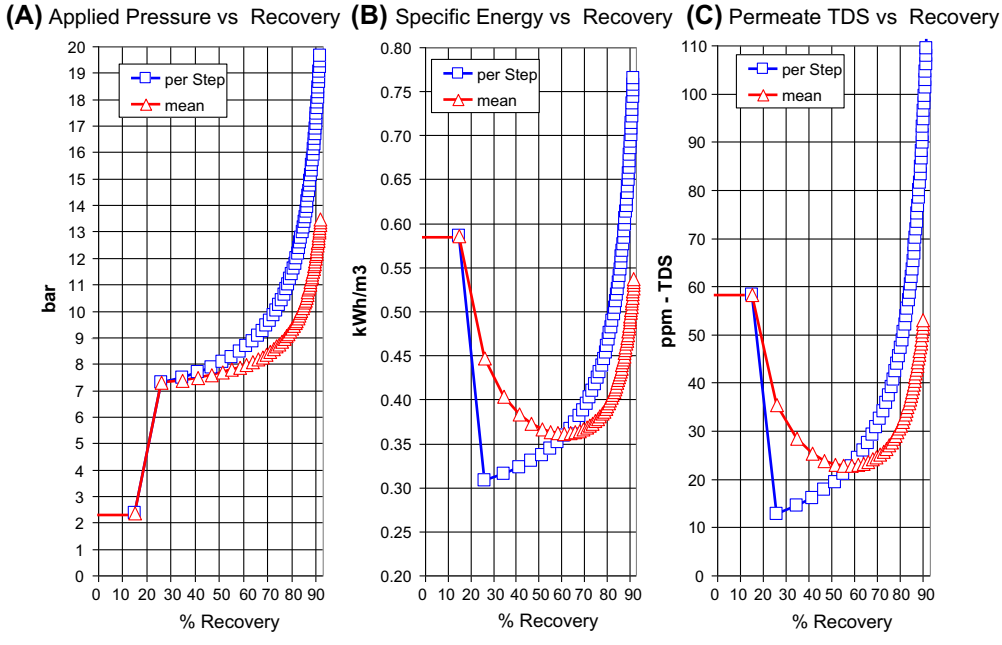

Fig. 6. Sequential batch variations of applied pressure (A), specific energy (B), and permeate TDS (C) during BWRO–CCD–PFD of 1,500 ppm NaCl according to the database in Table 3 with the single element (ESPA2 MAX) unit of the design displayed in Fig. 5.

10.8 → 2.3% in specific energy. In simple terms, the exemplified BWRO–CCD–PFD desalination of 0.15% NaCl if performed with 90% recovery using the simple apparatus depicted in Fig. 5 will require 5.6% greater specific energy and yield permeates of 10.4% higher average TDS compared the BWRO–CCD of near absolute energy efficiency performed by the more complex apparatus depicted in Fig. 2.

5. Discussion

CCD originated from theoretical considerations of a new conceptual model compared with conventional RO and ultimate experimental results are found to be within a relatively small error range (±4%) of the theoretical model predictions, and therefore the single element module simulations presented and discussed hereinabove appear both reliable and trustworthy. A noteworthy example in this context is the 4ME (*E* = SWC6) SWRO–CCD unit comprising four parallel single element modules, which was operated (25.5 ± 0.5˚C) with Mediterranean water (~4.1%) in the maximum pressure range of 60–72 bar of 40–52% desalination recovery in the element recovery range of 6–12% and the results of this operation revealed the exceptionally low RO specific energies displayed in Fig. 7(A) with extrapolation to ocean seawater of 3.5% displayed in Fig. 7(B). The extrapolated specific energy for ocean water desalination at flux of 13 according to Fig. 7(B) is 1.59 kWh/m^3 just above the simulate result of 1.57 kWh/m^3 in Table 1 for 50% recovery of 3.2% NaCl solution of near equivalent osmotic pressure to ocean seawater. The module's pressure difference and mean permeate conductivity vs. flux of said SWRO–CCD unit under the specified conditions are revealed in Fig. 8(A) and (B), respectively. The experimental pressure difference at 13 lmh in Fig. 8(A) of ~0.15 bar is within the error range of the calculated data (0.11 bar) in Table 1; whereas, the data of average permeate TDS in Fig. 8(B) pertain only to Mediterranean water without taking account of the exact system recovery and element recovery at each data point, and therefore the data in said figure does not allow a rigorous comparison with that in Table 1, although the overall trend is clear and consistent.

CCD applications of high recovery and low energy with reduced fouling characteristics were demonstrated thus far in the context of SWRO–CCD units of 1–4 [4,5,13] and 6 [17] elements per module and in BWRO–CCD and BWRO–CCD–PFD units of 3–4 [6–8] elements per module, and in each of the cases a good agreement was observed between the theoretically simulated and actual experimental results. Modules' size selection in CCD is a function of the desired recovery and the characteristics of the feed sources and their fouling constituents.

CCD can be performed with fixed flow under variable applied pressure and/or with fixed applied

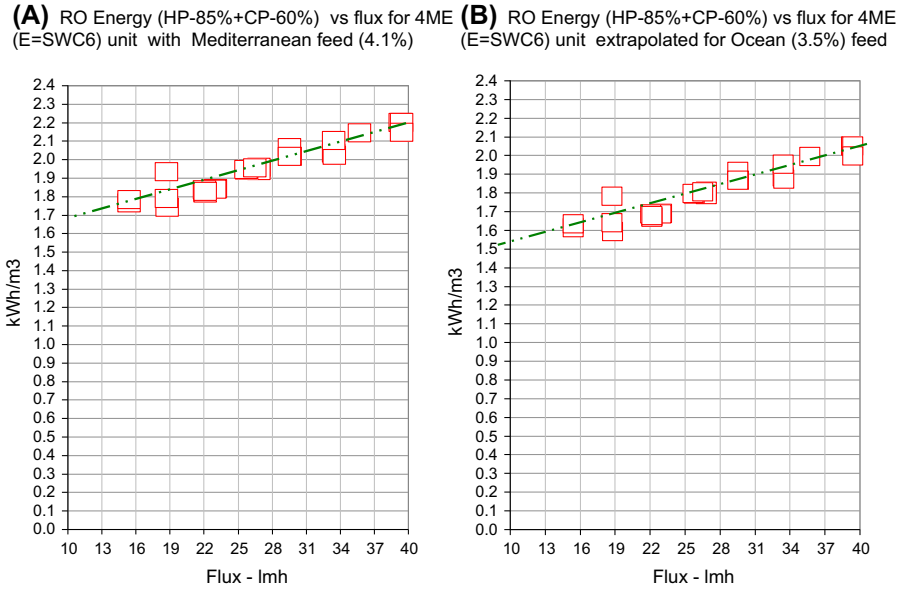

Fig. 7. RO energy vs. flux for the 4ME(E-SWC6) SWRO–CCD unit operation (25.5 + 0.5˚C) of 40–52% desalination recovery with Mediterranean water (4.1%) [A] in the element recovery range of 6–12%; maximum applied pressure rang of 60–72 bar; with 85% efficiency of HP; and 60% efficiency of CP and the extrapolated projections to ocean water (3.5%) (B).

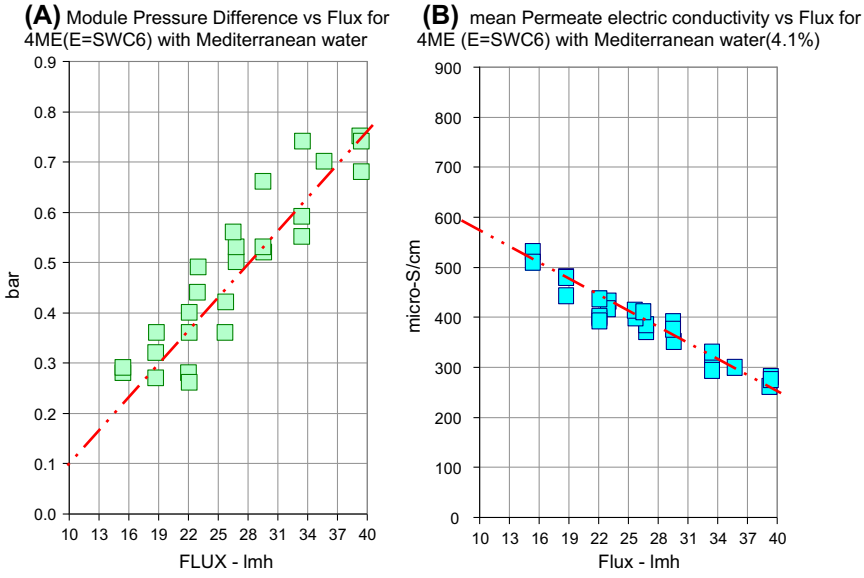

Fig. 8. Module pressure difference (A) and mean permeate conductivity (B) vs. flux encountered during the 4ME (E = SWC6) SWRO–CCD unit operation (25.5 ± 0.5°C) of 40–52% desalination recovery of Mediterranean water(4.1%) in the element recovery range of 6–12%; maximum applied pressure rang of 60–72 bar; 85% efficiency of HP; and 60% efficiency of CP.

pressure of declined flux conditions with infinite selection numbers of flow rates and pressure set points combinations for maximum process optimization of best possible results. Some performance characteristics and applications of single element modules CCD units are discussed next.

5.1. Low fouling aspects of CCD and of single element module in particular

Fouling of RO membranes arises from chemical damage (e.g. chlorine), suspended particulate matter in the feed in excess of a desire level (SDI < 5), films created by organic substances in the feed, bacteria growth on membrane surfaces, and scaling of low-solubility constituents when their solubility product (Ksp) is exceeded. Normal deterioration of RO membranes takes place as function of operational time as evident by an annual decline of flux with increased salt passage even under perfect conditions in the absence of distinct fouling factors which accelerate the wear down process. Front elements in RO modules show greater propensity to fouling by particulate matter and organic substance; whereas, tail elements are more prone to scaling with biofouling being initiated anywhere along the module of low cross flow, near constant salinity, and stable temperature conditions which stimulate bacteria growth and such conditions are generally found at the interphase of elements with pressure vessels. Membranes fouling by particulate matter and organic substances can be easily avoided by suitable pretreatment of feed (e.g. UF, MF, media filtration, activated carbon columns, etc.) with scaling and biofouling remaining the principle obstacle for uninterrupted durable BWRO operation.

In conventional BWRO as well as in BWRO–CCD performed with fixed flow under variable pressure conditions, each element operates with same average flux created by the same average NDP with unchanged salinity in the former case and large frequent salinity variations in the latter case. Controlled cross flow independent of controlled permeation flow, or flux, in case of BWRO–CCD, considered in the context of shorter modules of fewer elements compared with conventional BWRO, enables to create fast cross-flow of recycled concentrate with large frequent salinity variations of clear unfavorable conditions for bacteria growth. The propensity to biofouling in CCD declines in modules of lesser number of elements operated with declined module recovery of greater relative cross flow. CCD units of single element modules constitute an extreme case of high cross flow combined with frequent large salinity variations of exceptionally low propensity for the development of biofouling on membranes. In the illustrated performance of the BWRO–CCD ME unit in

Table 2, the average cross flow [$(2Q_{CP} + Q_{HP})/2$] of 6.29 m^3/h and permeation flow of 1.02 m^3/h are accompanied at 90% recovery with sequential salinity variations of 1,500 → 15,000 ppm NaCl every 14.35 min and much the same is also manifested by the performance of the BWRO–CCD–PFD ME unit in Table 3. Experience gained during the past 6 years with more than 40 installed CCD units consistently revealed minor, if any, biofouling indications even when feed to some of the units contained brackish water mixed with some domestic effluents from municipal sewage treatment plants and these findings clearly support the low biofouling characteristics of the CCD technology.

Scaling in BWRO occurs when the least soluble salt in the feed exceeds its solubility product (Ksp) at which point saturation is attained, and thereafter precipitation will take place and this dictates the recovery limitations of a given source. Increasing the recovery range of sources with scaling constituents such as $CaCO_3$, $CaSO_4$, $BaSO_4$, CaF_2, Silica, and others is achieved by means of anti-scaling agents, known as antiscalants, which enable the relevant ion constituents to remain in solution well beyond the Ksp of the pure salts. The use of highly effective antiscalants enables the attainment of higher recovery, although scaling inside the module will ultimately occur when the maximum allowed recovery level under such conditions is exceeded. Exceeding the maximum allowed recovery level in conventional BWRO normally takes place in the tail elements with rapid crystallization induced by high concentrations and a declined cross flow.

In contrast with conventional BWRO, the recycled concentrate in CCD is diluted with fresh feed at module's inlet causing scaling conditions develop only at the end of the last cycle of the consecutive sequential batch process of near maximum allowed recovery. After reaching maximum allowed recovery, the entire content of the closed circuit is flushed out, including minor amounts of crystalline scale if formed prior to this point. The last cycle of the of the consecutive sequential batch at maximum allowed recovery level is well characterized in the CCD process from the number of CCD cycles required to reach this level as defined by the Module Recovery (MR) [$MR = Q_{HP}/(Q_{HP} + Q_{CP}) = Q_P/(Q_P + Q_{CP})$] with greater number of cycles concomitant with lower MR in modules of fewer number of elements and vice versa. In theory, the largest number of cycles required to reach a maximum allowed recovery with CCD is attained with single element modules as is illustrated for ME in Tables 1–3. For example, attainment of 90% recovery with flux of 25 lmh by the BWRO–CCD–PFD ME unit described in Table 3 requires 50 cycles with MR = 15% (Q_{CP} = 5.78 m^3/h and Q_{HP} = 1.02 m^3/h) and if MR is changed to 13% by raising the flow rate of CP to 6.83 m^3/h, this will effect an increase in the number of cycles for 90% recovery to 59. Variations of module-recycled concentrates in this example (Table 3) on the recovery and CCD cycles scales are illustrated in Fig. 9(A) and (B), respectively, with an exponential curve revealed in the former and a linear curve in the latter. The moderating effects of CCD on scaling in a real feed source (e.g., 0.15%) of 90% recovery limits implies module concentrate outlet of 1.5% (15,000 ppm) as revealed in Fig. 9(B) at the end of the 50th CCD cycle with inlet and outlet concentrations during the 51st CCD cycle being 1.30 and 1.53%, respectively, however, if poly crystalline scaling is formed, it will be dissolved by mixing with fresh feed at the module inlet. The aforementioned implies that the process under review can proceed safely without rapid massive scaling as long as the minor amounts of the poly crystalline scaling particles are dissolved by dilution with fresh feed at the module inlet, and thereafter fast purge with fresh feed during the PFD step should dissolve and remove all the poly crystalline remains in the closed circuit, and thereby enable the start of a new consecutive sequential batch without any leftover remains from the preceding sequence. The flexible operation of CCD with selected set points of Q_{HP}, Q_{CP}, and maximum applied pressure, which are independent of each other, does enable the optimization of the process to avoid adverse scaling effects in a way not possible by any other RO technique.

5.2. Compact single element module(s) CCD unit(s) for common single-pass BWRO applications

The need for relatively small amounts of permeates arises in many RO applications and for this purpose all major membrane producers offer extensive lines of small-diameter membranes (4´´ and 2.5´´). Since CCD of a single element module can reach any desirable recovery made possible by the composition of the source with low energy consumption without need for ERD and without need for staging of pressure vessels as in case of the conventional RO, as already illustrated from the database in Tables 1–3, it means the availability of compact and efficient ME–CCD units of high flexibility for all the current RO applications which make use of 4´´ and 2.5´´ diameter elements and modules. For instance, a compact single element (8´´) BWRO–CCD ME unit apparatus (Fig. 2) with feed flow of 1.11 m^3/h operated under fixed flow and variable pressure conditions with 90% recovery according to the database in Table 2 will produce 1.0 m^3/h

Table 1
SWRO–CCD theoretical model simulation database of a single element (SWC6-MAX) unit operated under fixed flow and variable applied pressure conditions at 25°C, flux of 13 lmh, and element recovery of 10% with feed of 3.2% NaCl equivalent to typical ocean seawater of 35,000 ppm

TEST - SWC6 MAX		UNIT DESIGN		CCD Parameters		Temperature		
40.8	m2/Element	1	Modules	3.20	% Initial feed	≥25	25	°C
25	m3/day	1	Elements/Module	13.0	lmh Flux	≥25	1.000	TCF
32,000	ppm NaCl	130	cm long PV	0.53	m3/h Permeate (=Q_{HP})			
41	bar Applied Pressure	20	cm diameter PV	10	% Module Recovery	≤25	25	°C
10	% Recovery	15	liter element volume	4.77	m^3/h Qcp	≤25	1.000	TCF
25	Centig.	5	% lines volume	5.30	m^3/h Module Inlet flow			
99.50	% Salt Rejection	27.1	liter per module	0.11	bar Δp			
15.4	bar NDP			0.34	min/cycle CCD			
25.531	l/m2/h Flux	π(bar)-C(%)		0.0030	m3/cycle of permeate	Pumps		
1.6579	l/m2/h/bar -A	32,000	ppm NaCl Feed	0.100	av-MR/Element-CCD	0.85	HP *eff*.	
0.1002	l/m2/h - B	25.60	bar Osmotic Pressure	1.035	*av-pf* - CCD	0.75	CP *eff*.	
		8.00	π(bar)/C(%)	10.00	Flow ratio(concentrate/permeate)			

SWRO–CCD single element module performance

Cylce & concentrations				CCD sequence cycles							CCD sequence combined				Permeate	
					Applied (p_a)		Power (kW)			SE		Average		REC	Cycle	Average
Mode	Cycle	Inlet %	Outlet %	Time min	Bar	Av-bar	HP	CP	HP + CP	kWh/m3	Σm^3	ΣkW	kWh/m3	%	ppm	ppm
CCD	1	3.20	3.56	0.34	35.9	35.9	0.622	0.019	0.640	1.208	0.003	0.640	1.208	10.0	270	270
CCD	2	3.52	3.91	0.68	38.7	37.3	0.670	0.019	0.689	1.299	0.006	0.665	1.253	18.2	297	283
CCD	3	3.84	4.27	1.02	41.5	38.7	0.719	0.019	0.737	1.390	0.009	0.689	1.299	25.0	324	297
CCD	4	4.16	4.62	1.36	44.3	40.1	0.767	0.019	0.786	1.482	0.012	0.713	1.345	30.8	350	310
CCD	5	4.48	4.98	1.70	47.1	41.5	0.816	0.019	0.834	1.573	0.015	0.737	1.390	35.7	377	324
CCD	6	4.80	5.33	2.04	49.9	42.9	0.864	0.019	0.883	1.665	0.018	0.762	1.436	40.0	404	337
CCD	7	5.12	5.69	2.39	52.6	44.3	0.913	0.019	0.931	1.756	0.021	0.786	1.482	43.8	431	350
CCD	8	5.44	6.04	2.73	55.4	45.7	0.961	0.019	0.980	1.847	0.024	0.810	1.528	47.1	458	364
CCD	9	5.76	6.40	3.07	58.2	47.1	1.010	0.019	1.028	1.939	0.027	0.834	1.573	50.0	485	377
CCD	10	6.08	6.76	3.41	61.0	48.5	1.058	0.019	1.077	2.030	0.030	0.859	1.619	52.6	512	391
CCD	11	6.40	7.11	3.75	63.8	49.9	1.107	0.019	1.125	2.122	0.033	0.883	1.665	55.0	539	404
CCD	12	6.72	7.47	4.09	66.6	51.3	1.155	0.019	1.174	2.213	0.036	0.907	1.710	57.1	566	418
CCD	13	7.04	7.82	4.43	69.4	52.6	1.203	0.019	1.222	2.304	0.039	0.931	1.756	59.1	593	431
CCD	14	7.36	8.18	4.77	72.2	54.0	1.252	0.019	1.271	2.396	0.042	0.956	1.802	60.9	620	445
A1	A2	A3	A4	A5	A6	A7	A8	A9	A10	A11	A12	A13	A14	A15	A16	A17

Notes: Temperature ≥ 25°C TCF = EXP[**2,640**(1/298 − 1/(273 + C)]; Temperature ≤ 25°C TCF = EXP[**3,020**(1/298 − 1/(273 + C)].

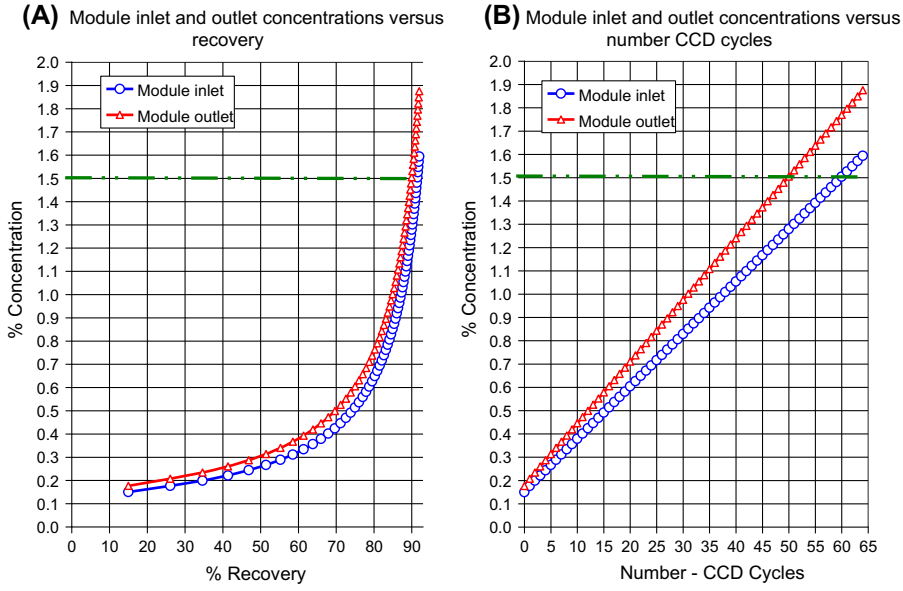

Fig. 9. Module inlet and outlet concentrations vs. % recovery (A) and number of CCD cycles (B) in database for the BWRO–CCD–PFD ME unit described in Table 3.

permeates; whereas, the same permeate flow with the same recovery by conventional BWRO will necessitate a 4:2:1 staged vessels design with 8 elements per vessel and three-fold more components if the selected elements are of 2.5′′ diameter. Essentially the same comparative results shall be attainable also with the less complex BWRO–CCD–PFD ME unit design apparatus displayed in Fig. 5. Apart from significant savings in components, the compact CCD units under review will operate with greater flexibility and lower energy consumption with reduced fouling characteristics compared with the small-diameter conventional RO apparatus for equivalent permeate flow production. The aforementioned implies the clear advantage of small compact CCD units over conventional units.

5.3. Compact single element module(s) CCD unit(s) for common double-pass BWRO applications

The need for relatively small amounts of high quality permeates also arise in many RO applications and for this purpose single element module(s) units of the design displayed in Fig. 5 could be made to perform a 2nd pass according to the scheme in Fig. 10(A)–(B) by adding to the basic design an intermediary permeate collection tank (T10) and valve means (V11, V12, V21 and V22). The operation of the system proceeds by the desalination of the source with valve means as displayed in Fig. 10(A) with 1st pass permeates collected in T10 and when the recovery level is reached, the system is switched to the desalination of the 1st permeates in T10 instead of the source according to the scheme in Fig. 10(B) with high quality permeates collected in T20. When the desired TDS of the 2nd pass permeates is exceeded, the system will revert back to its first mode of operation (Fig. 10(A)). The entire system is operated through its control board by means of monitored data of flow and conductivity and set points of the desired process parameters. The aforementioned illustrates how a single element module apparatus could be made to perform both 1st and 2nd passes to yield high quality permeates without need of staged pressure vessels designs of many elements of as would be required to perform the same by conventional RO techniques.

5.4. Compact single element module(s) CCD unit(s) for medical dialysis applications

Application of BWRO for medical dialysis which is practiced in millions of sites worldwide, including hospital, clinics, dialysis centers, and private places, represents an important example of a major small-scale RO application. Most dialysis services require small RO units (1–5 m^3/h) and are operated 24 h/d. RO dialysis units normally operate with ~50% recovery with discharge brine drained in order to meet the low TDS requirements of permeates. Drainage of low recovery RO brine implies in many parts of the world large losses of expensive potable water. For instance,

Table 2
BWRO–CCD theoretical model simulation database of a single element (ESPA2-MAX) unit operated under fixed flow of variable applied pressure conditions at 25℃, flux of 25 lmh, and element recovery of 15% with feed of 1,500 ppm NaCl typical of common brackish water sources of 1,700—2,000 ppm TDS depending on their specific compositions

TEST - ESPA2 MAX-8O40≈≈		UNIT DESIGN		CCD Parameters		Temperature		
40.8	m2/Element	1	Modules	0.15	% Initial feed	≥25	25	°C
45.4	m3/day	1	Elements/Module	25.0	lmh Flux	≥25	1.000	TCF
1,500	ppm NaCl	130	cm long PV	1.02	m3/h Permeate (=Q_{HP})			
10.5	bar Applied Pressure	20	cm diameter PV	15	% Module Recovery	≤25	25	°C
15	% Recovery	15	liter element volume	5.78	m^3/h Qcp	≤25	1.000	TCF
25	Centig.	5	% lines volume	6.80	m^3/h Module Inlet flow			
99.60	% Salt Rejection	27.1	liter per module	0.15	bar Δp			
9.3	bar NDP			0.28	min/cycle CCD			
46.364	l/m2/h Flux	π(bar)-C(%)		0.0048	m3/cycle of permeate	Pumps		
4.9854	l/m2/h/bar -A	1,500	ppm NaCl Feed	0.150	av-Element Recovery-CCD	0.75	HP *eff*.	
0.1456	l/m2/h - B	1.20	bar Osmotic Pressure	1.053	*av-pf* - CCD	0.75	CP *eff*.	
		8.00	π(bar)/C(%)	6.67	Flow ratio(concentrate/permeate)			

Steps & concentrations				CCD sequence cycles							CCD sequence combined				Permeate	
					Applied (p_a)		Power (kW)			SE		Average		REC	Cycle	Average
Mode	Cycle	Inlet %	Outlet %	Time min	Bar	Av-bar	HP	CP	HP + CP	kWh/m3	Σm^3	ΣkW	kWh/m3	%	ppm	ppm
CCD	1	0.15	0.18	0.28	6.5	6.5	0.244	0.032	0.277	0.271	0.005	0.277	0.271	15.0	10	10
CCD	2	0.17	0.20	0.56	6.7	6.6	0.252	0.032	0.285	0.279	0.010	0.281	0.275	26.1	12	11
CCD	3	0.20	0.23	0.84	6.9	6.7	0.260	0.032	0.292	0.287	0.014	0.285	0.279	34.6	13	12
CCD	4	0.22	0.26	1.13	7.1	6.8	0.268	0.032	0.300	0.294	0.019	0.288	0.283	41.4	15	12
CCD	5	0.24	0.28	1.41	7.3	6.9	0.275	0.032	0.308	0.302	0.024	0.292	0.287	46.9	16	13
CCD	6	0.26	0.31	1.69	7.5	7.0	0.283	0.032	0.316	0.310	0.029	0.296	0.290	51.4	18	14
CCD	7	0.29	0.34	1.97	7.7	7.1	0.291	0.032	0.323	0.317	0.033	0.300	0.294	55.3	19	15
CCD	8	0.31	0.36	2.25	7.9	7.2	0.299	0.032	0.331	0.325	0.038	0.304	0.298	58.5	21	15
CCD	9	0.33	0.39	2.53	8.1	7.3	0.307	0.032	0.339	0.332	0.043	0.308	0.302	61.4	22	16
CCD	10	0.35	0.41	2.81	8.3	7.4	0.314	0.032	0.347	0.340	0.048	0.312	0.306	63.8	24	17
CCD	11	0.38	0.44	3.10	8.5	7.5	0.322	0.032	0.355	0.348	0.053	0.316	0.310	66.0	25	18
CCD	12	0.40	0.47	3.38	8.7	7.6	0.330	0.032	0.362	0.355	0.057	0.320	0.313	67.9	27	18
CCD	13	0.42	0.49	3.66	8.9	7.7	0.338	0.032	0.370	0.363	0.062	0.323	0.317	69.6	28	19
CCD	14	0.44	0.52	3.94	9.1	7.8	0.346	0.032	0.378	0.371	0.067	0.327	0.321	71.2	30	20
CCD	15	0.47	0.55	4.22	9.4	7.9	0.353	0.032	0.386	0.378	0.072	0.331	0.325	72.6	31	21
CCD	16	0.49	0.57	4.50	9.6	8.0	0.361	0.032	0.394	0.386	0.077	0.335	0.329	73.8	33	21
CCD	17	0.51	0.60	4.78	9.8	8.1	0.369	0.032	0.401	0.394	0.081	0.339	0.332	75.0	34	22
CCD	18	0.53	0.63	5.07	10.0	8.2	0.377	0.032	0.409	0.401	0.086	0.343	0.336	76.1	36	23
CCD	19	0.56	0.65	5.35	10.2	8.3	0.385	0.032	0.417	0.409	0.091	0.347	0.340	77.0	37	24
CCD	20	0.58	0.68	5.63	10.4	8.4	0.392	0.032	0.425	0.416	0.096	0.351	0.344	77.9	39	24

(*Continued*)

Table 2 (*Continued*)

Steps & concentrations				CCD sequence cycles							CCD sequence combined				Permeate	
					Applied (p_a)		Power (kW)					Average				
Mode	Cycle	Inlet %	Outlet %	Time min	Bar	Av-bar	HP	CP	HP + CP	SE kWh/m3	Σm^3	ΣkW	kWh/m3	REC %	Cycle ppm	Average ppm
CCD	21	0.60	0.71	5.91	10.6	8.5	0.400	0.032	0.433	0.424	0.100	0.355	0.348	78.8	40	25
CCD	22	0.62	0.73	6.19	10.8	8.6	0.408	0.032	0.440	0.432	0.105	0.359	0.352	79.5	42	26
CCD	23	0.65	0.76	6.47	11.0	8.7	0.416	0.032	0.448	0.439	0.110	0.362	0.355	80.2	43	27
CCD	24	0.67	0.79	6.75	11.2	8.8	0.424	0.032	0.456	0.447	0.115	0.366	0.359	80.9	45	27
CCD	25	0.69	0.81	7.04	11.4	8.9	0.431	0.032	0.464	0.455	0.120	0.370	0.363	81.5	46	28
CCD	26	0.71	0.84	7.32	11.6	9.0	0.439	0.032	0.472	0.462	0.124	0.374	0.367	82.1	48	29
CCD	27	0.74	0.86	7.60	11.8	9.1	0.447	0.032	0.479	0.470	0.129	0.378	0.371	82.7	49	30
CCD	28	0.76	0.89	7.88	12.0	9.3	0.455	0.032	0.487	0.478	0.134	0.382	0.374	83.2	51	30
CCD	29	0.78	0.92	8.16	12.2	9.4	0.462	0.032	0.495	0.485	0.139	0.386	0.378	83.7	52	31
CCD	30	0.80	0.94	8.44	12.4	9.5	0.470	0.032	0.503	0.493	0.144	0.390	0.382	84.1	54	32
CCD	31	0.83	0.97	8.72	12.7	9.6	0.478	0.032	0.511	0.501	0.148	0.394	0.386	84.5	55	33
CCD	32	0.85	1.00	9.01	12.9	9.7	0.486	0.032	0.518	0.508	0.153	0.398	0.390	85.0	57	33
CCD	33	0.87	1.02	9.29	13.1	9.8	0.494	0.032	0.526	0.516	0.158	0.401	0.394	85.3	58	34
CCD	34	0.89	1.05	9.57	13.3	9.9	0.501	0.032	0.534	0.523	0.163	0.405	0.397	85.7	60	35
CCD	35	0.92	1.08	9.85	13.5	10.0	0.509	0.032	0.542	0.531	0.167	0.409	0.401	86.1	61	36
CCD	36	0.94	1.10	10.13	13.7	10.1	0.517	0.032	0.550	0.539	0.172	0.413	0.405	86.4	63	36
CCD	37	0.96	1.13	10.41	13.9	10.2	0.525	0.032	0.557	0.546	0.177	0.417	0.409	86.7	64	37
CCD	38	0.98	1.16	10.69	14.1	10.3	0.533	0.032	0.565	0.554	0.182	0.421	0.413	87.0	66	38
CCD	39	1.01	1.18	10.98	14.3	10.4	0.540	0.032	0.573	0.562	0.187	0.425	0.416	87.3	67	39
CCD	40	1.03	1.21	11.26	14.5	10.5	0.548	0.032	0.581	0.569	0.191	0.429	0.420	87.6	69	39
CCD	41	1.05	1.24	11.54	14.7	10.6	0.556	0.032	0.588	0.577	0.196	0.433	0.424	87.9	70	40
CCD	42	1.07	1.26	11.82	14.9	10.7	0.564	0.032	0.596	0.585	0.201	0.437	0.428	88.1	72	41
CCD	43	1.10	1.29	12.10	15.1	10.8	0.572	0.032	0.604	0.592	0.206	0.440	0.432	88.4	73	42
CCD	44	1.12	1.31	12.38	15.3	10.9	0.579	0.032	0.612	0.600	0.211	0.444	0.436	88.6	75	42
CCD	45	1.14	1.34	12.66	15.5	11.0	0.587	0.032	0.620	0.607	0.215	0.448	0.439	88.8	76	43
CCD	46	1.16	1.37	12.95	15.7	11.1	0.595	0.032	0.627	0.615	0.220	0.452	0.443	89.0	78	44
CCD	47	1.19	1.39	13.23	16.0	11.2	0.603	0.032	0.635	0.623	0.225	0.456	0.447	89.2	79	45
CCD	48	1.21	1.42	13.51	16.2	11.3	0.611	0.032	0.643	0.630	0.230	0.460	0.451	89.4	81	45
CCD	49	1.23	1.45	13.79	16.4	11.4	0.618	0.032	0.651	0.638	0.234	0.464	0.455	89.6	82	46
CCD	50	1.25	1.47	14.07	16.6	11.5	0.626	0.032	0.659	0.646	0.239	0.468	0.459	89.8	84	47
CCD	51	1.28	1.50	14.35	16.8	11.6	0.634	0.032	0.666	0.653	0.244	0.472	0.462	90.0	85	48
CCD	52	1.30	1.53	14.63	17.0	11.7	0.642	0.032	0.674	0.661	0.249	0.475	0.466	90.2	87	48
CCD	53	1.32	1.55	14.92	17.2	11.8	0.650	0.032	0.682	0.669	0.254	0.479	0.470	90.3	88	49
CCD	54	1.34	1.58	15.20	17.4	11.9	0.657	0.032	0.690	0.676	0.258	0.483	0.474	90.5	90	50
CCD	55	1.37	1.61	15.48	17.6	12.0	0.665	0.032	0.698	0.684	0.263	0.487	0.478	90.7	91	51
CCD	56	1.39	1.63	15.76	17.8	12.1	0.673	0.032	0.705	0.692	0.268	0.491	0.481	90.8	93	51
CCD	57	1.41	1.66	16.04	18.0	12.2	0.681	0.032	0.713	0.699	0.273	0.495	0.485	91.0	94	52
CCD	58	1.43	1.69	16.32	18.2	12.3	0.688	0.032	0.721	0.707	0.277	0.499	0.489	91.1	96	53
CCD	59	1.46	1.71	16.60	18.4	12.4	0.696	0.032	0.729	0.714	0.282	0.503	0.493	91.2	97	54
CCD	60	1.48	1.74	16.89	18.6	12.6	0.704	0.032	0.737	0.722	0.287	0.507	0.497	91.4	99	54

Table 3
BWRO–CCD–PFD theoretical model simulation database of a single element (ESPA2-MAX) unit operated most of the time at 25°C with feed of 1,500 ppm NaCl under CCD conditions of 25 lmh and 15% element recovery and part of the time under PFD conditions of 4.7 lmh and 15% element recovery with 25% greater feed flow compared with CCD

Test -ESPA2 MAX		Unit Design		PFD		CCD		General Information	
40.8	m^2/Element	1	Modules	0.150	% NaCl	0.18	% Initial feed	0.15	av-Elem. Rec. PFD
45.4	m^3/day	1	Elements/Module	25	% increased HP flow	25.0	lmh Flux	0.15	av-Elem. Rec. CCD
1,500	ppm NaCl	130	cm long PV	1.28	m^3/h Feed PFD	15	% Module Recovery CCD	1.1482	*av-pf* - PFD
10.5	bar Applied Pressure	20	cm diameter PV	15	% Recovery PFD	0.18	bar Δp CCD	1.1482	*av-pf* - CCD
15	% Recovery	5	% added conduits	0.01	bar Δp PFD	1.02	m^3/h Permeate (=Q_{HP})		
25	°C	15	liter per element	0.19	m^3/h Permeate PFD	5.78	m^3/h Qcp CCD	PUMPS	
99.6	% Salt Rejection	27.1	liter per module	1.08	m^3/h Brine PFD	0.28	min/cycle CCD	0.75	HP Eff.
9.285	bar NDP			0.18	% Brine PFD	0.0048	m3/Cycle CCD	0.75	CP Eff.
46.36	l/m^2/h Flux			4.7	lmh flux				
4.416	l/m^2/h/bar -A			1.501	min/step PDF			TEMPERATURE	
0.146	l/m^2/h - B			0.005	m^3/step Permeate PFD			25	°C
8.00	π(bar)/C(%) - assumed			2.4	bar Applied Pressure PFD			1.000	TCF

ME4 module data				Separate CCD cycles & PFD step							Combined sequence (CCD cycles & PFD Step)					Permeate		
												Permeate - m^3			Energy			
Mode	Step	Inlet %	Outlet %	Time min	p_{appl} Bar	Av-p_{appl} Bar	HP kW	CP kW	HP + CP kW	Per step kWh/m3	Time Σmin	Step	Σm3	REC %	ΣkWh	kWh/m^3	Step ppm	Mean ppm
PFD	0	0.15	0.18	1.50	2.4	2.4	0.112	0.000	0.112	0.586	1.5	0.005	0.005	15.0	0.003	0.586	58	58
CCD	1	0.18	0.21	0.28	7.3	7.3	0.275	0.039	0.314	0.308	1.8	0.005	0.010	26.1	0.004	0.447	13	36
CCD	2	0.20	0.23	0.56	7.5	7.4	0.283	0.039	0.322	0.315	2.1	0.005	0.014	34.6	0.006	0.403	14	29
CCD	3	0.22	0.26	0.84	7.7	7.5	0.290	0.039	0.329	0.323	2.3	0.005	0.019	41.4	0.007	0.383	16	25
CCD	4	0.24	0.29	1.13	7.9	7.6	0.298	0.039	0.337	0.330	2.6	0.005	0.024	46.9	0.009	0.372	18	24
CCD	5	0.27	0.31	1.41	8.1	7.7	0.305	0.039	0.344	0.337	2.9	0.005	0.029	51.4	0.011	0.367	19	23
CCD	6	0.29	0.34	1.69	8.3	7.8	0.312	0.039	0.351	0.345	3.2	0.005	0.033	55.3	0.012	0.363	21	23
CCD	7	0.31	0.37	1.97	8.5	7.9	0.320	0.039	0.359	0.352	3.5	0.005	0.038	58.5	0.014	0.362	23	23
CCD	8	0.33	0.39	2.25	8.7	8.0	0.327	0.039	0.366	0.359	3.8	0.005	0.043	61.4	0.016	0.362	24	23
CCD	9	0.36	0.42	2.53	8.9	8.1	0.335	0.039	0.374	0.366	4.0	0.005	0.048	63.8	0.017	0.362	26	23
CCD	10	0.38	0.45	2.81	9.1	8.2	0.342	0.039	0.381	0.374	4.3	0.005	0.053	66.0	0.019	0.363	28	24
CCD	11	0.40	0.47	3.10	9.2	8.3	0.349	0.039	0.388	0.381	4.6	0.005	0.057	67.9	0.021	0.365	29	24
CCD	12	0.42	0.50	3.38	9.4	8.4	0.357	0.039	0.396	0.388	4.9	0.005	0.062	69.6	0.023	0.366	31	25
CCD	13	0.45	0.53	3.66	9.6	8.5	0.364	0.039	0.403	0.395	5.2	0.005	0.067	71.2	0.025	0.368	32	25
CCD	14	0.47	0.55	3.94	9.8	8.6	0.372	0.039	0.411	0.403	5.4	0.005	0.072	72.6	0.027	0.371	34	26
CCD	15	0.49	0.58	4.22	10.0	8.7	0.379	0.039	0.418	0.410	5.7	0.005	0.077	73.8	0.029	0.373	36	26
CCD	16	0.51	0.60	4.50	10.2	8.8	0.386	0.039	0.425	0.417	6.0	0.005	0.081	75.0	0.031	0.376	37	27
CCD	17	0.54	0.63	4.78	10.4	8.9	0.394	0.039	0.433	0.424	6.3	0.005	0.086	76.1	0.033	0.378	39	28
CCD	18	0.56	0.66	5.07	10.6	9.0	0.401	0.039	0.440	0.432	6.6	0.005	0.091	77.0	0.035	0.381	41	28
CCD	19	0.58	0.68	5.35	10.8	9.1	0.409	0.039	0.448	0.439	6.8	0.005	0.096	77.9	0.037	0.384	42	29
CCD	20	0.60	0.71	5.63	11.0	9.2	0.416	0.039	0.455	0.446	7.1	0.005	0.100	78.8	0.039	0.387	44	30
CCD	21	0.63	0.74	5.91	11.2	9.2	0.423	0.039	0.462	0.453	7.4	0.005	0.105	79.5	0.041	0.390	46	31

(*Continued*)

Table 3 (*Continued*)

ME4 module data				Separate CCD cycles & PFD step							Combined sequence (CCD cycles & PFD Step)					Permeate		
												Permeate - m^3			Energy			
Mode	Step	Inlet %	Outlet %	Time min	p_{appl} Bar	Av-p_{appl} Bar	HP kW	CP kW	HP + CP kW	Per step kWh/m3	Time Σmin	Step	Σm3	REC %	ΣkWh	kWh/m^3	Step ppm	Mean ppm
CCD	22	0.65	0.76	6.19	11.4	9.3	0.431	0.039	0.470	0.461	7.7	0.005	0.110	80.2	0.043	0.393	47	31
CCD	23	0.67	0.79	6.47	11.6	9.4	0.438	0.039	0.477	0.468	8.0	0.005	0.115	80.9	0.046	0.396	49	32
CCD	24	0.69	0.82	6.75	11.8	9.5	0.446	0.039	0.485	0.475	8.3	0.005	0.120	81.5	0.048	0.399	51	33
CCD	25	0.72	0.84	7.04	12.0	9.6	0.453	0.039	0.492	0.482	8.5	0.005	0.124	82.1	0.050	0.403	52	33
CCD	26	0.74	0.87	7.32	12.2	9.7	0.460	0.039	0.499	0.490	8.8	0.005	0.129	82.7	0.052	0.406	54	34
CCD	27	0.76	0.90	7.60	12.4	9.8	0.468	0.039	0.507	0.497	9.1	0.005	0.134	83.2	0.055	0.409	55	35
CCD	28	0.78	0.92	7.88	12.6	9.9	0.475	0.039	0.514	0.504	9.4	0.005	0.139	83.7	0.057	0.412	57	36
CCD	29	0.81	0.95	8.16	12.8	10.0	0.483	0.039	0.522	0.511	9.7	0.005	0.144	84.1	0.060	0.416	59	37
CCD	30	0.83	0.98	8.44	13.0	10.1	0.490	0.039	0.529	0.519	9.9	0.005	0.148	84.5	0.062	0.419	60	37
CCD	31	0.85	1.00	8.72	13.2	10.2	0.497	0.039	0.536	0.526	10.2	0.005	0.153	85.0	0.065	0.422	62	38
CCD	32	0.87	1.03	9.01	13.4	10.3	0.505	0.039	0.544	0.533	10.5	0.005	0.158	85.3	0.067	0.426	64	39
CCD	33	0.90	1.05	9.29	13.6	10.4	0.512	0.039	0.551	0.540	10.8	0.005	0.163	85.7	0.070	0.429	65	40
CCD	34	0.92	1.08	9.57	13.8	10.5	0.520	0.039	0.559	0.548	11.1	0.005	0.167	86.1	0.072	0.432	67	40
CCD	35	0.94	1.11	9.85	13.9	10.6	0.527	0.039	0.566	0.555	11.4	0.005	0.172	86.4	0.075	0.436	69	41
CCD	36	0.96	1.13	10.13	14.1	10.7	0.534	0.039	0.573	0.562	11.6	0.005	0.177	86.7	0.078	0.439	70	42
CCD	37	0.99	1.16	10.41	14.3	10.8	0.542	0.039	0.581	0.569	11.9	0.005	0.182	87.0	0.080	0.443	72	43
CCD	38	1.01	1.19	10.69	14.5	10.9	0.549	0.039	0.588	0.577	12.2	0.005	0.187	87.3	0.083	0.446	73	44
CCD	39	1.03	1.21	10.98	14.7	11.0	0.557	0.039	0.596	0.584	12.5	0.005	0.191	87.6	0.086	0.450	75	44
CCD	40	1.05	1.24	11.26	14.9	11.1	0.564	0.039	0.603	0.591	12.8	0.005	0.196	87.9	0.089	0.453	77	45
CCD	41	1.08	1.27	11.54	15.1	11.2	0.571	0.039	0.610	0.598	13.0	0.005	0.201	88.1	0.092	0.456	78	46
CCD	42	1.10	1.29	11.82	15.3	11.3	0.579	0.039	0.618	0.606	13.3	0.005	0.206	88.4	0.095	0.460	80	47
CCD	43	1.12	1.32	12.10	15.5	11.4	0.586	0.039	0.625	0.613	13.6	0.005	0.211	88.6	0.098	0.463	82	47
CCD	44	1.14	1.35	12.38	15.7	11.5	0.594	0.039	0.633	0.620	13.9	0.005	0.215	88.8	0.101	0.467	83	48
CCD	45	1.17	1.37	12.66	15.9	11.6	0.601	0.039	0.640	0.627	14.2	0.005	0.220	89.0	0.104	0.470	85	49
CCD	46	1.19	1.40	12.95	16.1	11.7	0.608	0.039	0.647	0.635	14.4	0.005	0.225	89.2	0.107	0.474	87	50
CCD	47	1.21	1.43	13.23	16.3	11.8	0.616	0.039	0.655	0.642	14.7	0.005	0.230	89.4	0.110	0.477	88	51
CCD	48	1.23	1.45	13.51	16.5	11.9	0.623	0.039	0.662	0.649	15.0	0.005	0.234	89.6	0.113	0.481	90	51
CCD	49	1.26	1.48	13.79	16.7	12.0	0.631	0.039	0.670	0.656	15.3	0.005	0.239	89.8	0.116	0.484	91	52
CCD	50	1.28	1.50	14.07	16.9	12.1	0.638	0.039	0.677	0.664	15.6	0.005	0.244	90.0	0.119	0.488	93	53
CCD	51	1.30	1.53	14.35	17.1	12.2	0.645	0.039	0.684	0.671	15.9	0.005	0.249	90.2	0.122	0.491	95	54
CCD	52	1.32	1.56	14.63	17.3	12.3	0.653	0.039	0.692	0.678	16.1	0.005	0.254	90.3	0.126	0.495	96	55
CCD	53	1.35	1.58	14.92	17.5	12.4	0.660	0.039	0.699	0.685	16.4	0.005	0.258	90.5	0.129	0.499	98	55
CCD	54	1.37	1.61	15.20	17.7	12.5	0.668	0.039	0.707	0.693	16.7	0.005	0.263	90.7	0.132	0.502	100	56
CCD	55	1.39	1.64	15.48	17.9	12.6	0.675	0.039	0.714	0.700	17.0	0.005	0.268	90.8	0.135	0.506	101	57
CCD	56	1.41	1.66	15.76	18.1	12.7	0.682	0.039	0.721	0.707	17.3	0.005	0.273	91.0	0.139	0.509	103	58
CCD	57	1.44	1.69	16.04	18.3	12.8	0.690	0.039	0.729	0.715	17.5	0.005	0.277	91.1	0.142	0.513	105	59
CCD	58	1.46	1.72	16.32	18.5	12.9	0.697	0.039	0.736	0.722	17.8	0.005	0.282	91.2	0.146	0.516	106	59
CCD	59	1.48	1.74	16.60	18.7	13.0	0.705	0.039	0.744	0.729	18.1	0.005	0.287	91.4	0.149	0.520	108	60
CCD	60	1.50	1.77	16.89	18.8	13.1	0.712	0.039	0.751	0.736	18.4	0.005	0.292	91.5	0.153	0.523	109	61
CCD	61	1.53	1.80	17.17	19.0	13.2	0.719	0.039	0.758	0.744	18.7	0.005	0.297	91.6	0.156	0.527	111	62
CCD	62	1.55	1.82	17.45	19.2	13.3	0.727	0.039	0.766	0.751	18.9	0.005	0.301	91.7	0.160	0.530	113	63
CCD	63	1.57	1.85	17.73	19.4	13.4	0.734	0.039	0.773	0.758	19.2	0.005	0.306	91.9	0.163	0.534	114	64
CCD	64	1.59	1.88	18.01	19.6	13.5	0.742	0.039	0.781	0.765	19.5	0.005	0.311	92.0	0.167	0.538	116	64

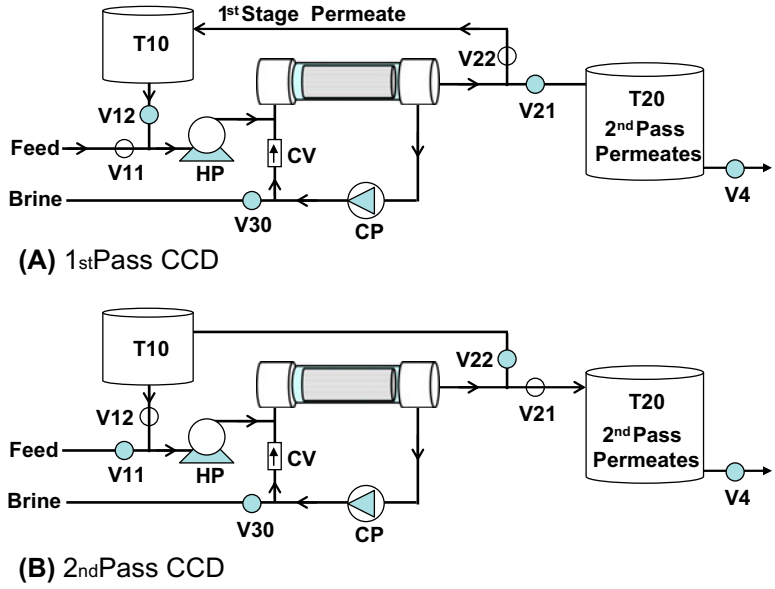

Fig. 10. A schematic design of a single element module BWRO–CCD system for performing both 1st (A) and 2nd (B) pass alternately—the features in the drawing are identified in the same manner as described elsewhere hereinabove.

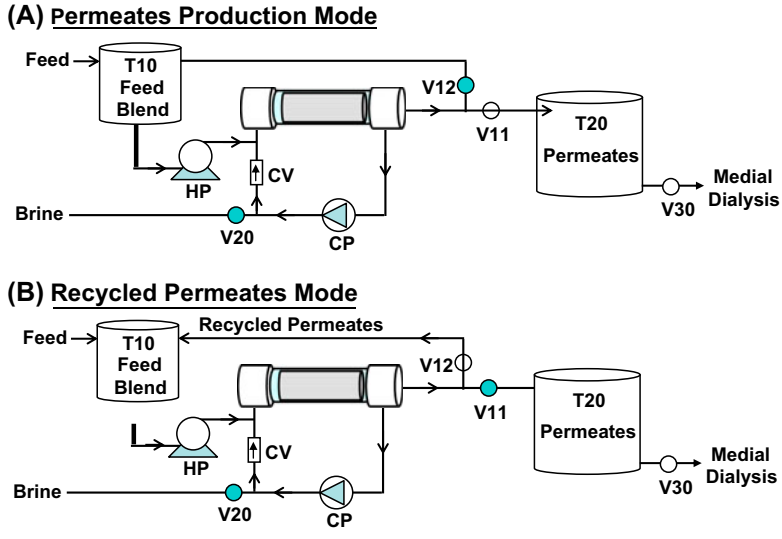

Fig. 11. A schematic design of a single element module BWRO–CCD system for medical dialysis with high recovery permeates of low TDS with permeates production mode (A) and permeate recycling mode (B)—the features in the drawing are identified in the same manner as described elsewhere hereinabove.

average price of potable water in Israel is ~2.5 $/m^3 and this implies that a typical dialysis center with RO unit of 4.0 m^3/h operated around the clock with 50% recovery will drain the equivalent of 120 $/d (3,600 $/month and 43,200 $/y), and therefore the savings of lost water becomes an economical issue. The BWRO–CCD–PFD technology enables construction of inexpensive small compact units of high recovery for permeates of low TDS for medical dialysis applications according to the illustrated schematic design of the single element unit in Fig. 11. The exemplified unit with common electric conductivity (EC) monitoring

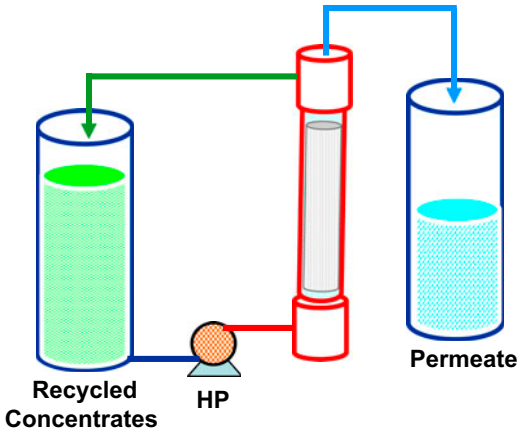

Fig. 12. A single element module SWRO batch apparatus for volume reduction of concentrates [18] with its high pressure pump (HP) and tanks of recycled concentrates and permeate.

means will divert permeates with EC under a desired maximum set point to the supply container for medical dialysis (T20) according to the illustration in Fig. 11(A) and when the EC of permeates exceeds the desired maximum level, they will be recycled to the blend container (T10) according to Fig. 11(B), mix with fresh feed, and thereby reduce the feed salinity to HP and lead to better quality permeates. In simple terms, the recycled permeate to the blend container will affect the production of better quality permeate with a higher overall recovery, and therefore save significantly on costs of fresh water.

5.5. Compact single element module(s) CCD unit(s) for volume reduction of concentrates and industrial effluents

CCD with units comprising single element modules of versatile flexible control could be found highly effective for volume reduction of concentrates and industrial effluents. A recent US patent application [18] entitled "Sea water reverse osmosis system to reduce concentrate volume prior to disposal" describes an open-circuit batch SWRO pilot comprising a single membrane element of the schematic design in Fig. 12 for 80–85% volume reduction of concentrates derived from a BWRO plant of 80% recovery of the average composition in 2009 (unless indicated otherwise in parenthesis) of Na, 2,810; K, 113; Ca, 606; Mg, 161; Ba, 0.31(2007); Sr, 17.1(2007); Fe, 0.07; Mn, 0.17; Cl, 5,089; SO_4, 1,111; SiO_2, 131; TDS, 10,722 ppm; EC, 18,122 μS/cm; pH, 7.8; turbidity, 0.3; and temperature 25.4˚C. The overall water recovery achieved during the combined BWRO (80%) and SWRO (80–85%) processes was in the range of 96–97%. The SWRO process was carried out at pH of 3–5 at constant applied pressure of 700–740 psi created by a high pressure pump (HP) with feed drawn from the recycled concentrate tank and permeate delivered to the permeate tank. The batch process was carried out in the presence of an effective antiscalant under declined flux conditions with percent reduction of volume determined by the duration of the batch sequence. According to the reported trial results [18], the super-concentrates created during the process remained clear and did not cause fouling, and a brief rinse out of the membrane at the end of each batch was sufficient to restore the initial flux in the proceeding batch trial.

While the focus in the aforementioned study was on super-saturated silica concentrates in excess of 1,000 ppm, the fact that none of the other constituents precipitated and the treated super-concentrates (TDS range: 10,000—60,000 ppm) remained clear during the entire process may suggest that low pH batch SWRO under declined flux conditions using single element modules could be highly effective for volume reduction of great many industrial effluents apart from BWRO brine concentrates. In this context, the CCD single element module apparatus of the types displayed in Figs. 2 and 5 and alike, with more than one such module, could be ideal for volume reduction of industrial effluents by a process which also enables the reuse of rescued water. The prospects for extensive concentrate volume reduction by CCD are based on the already established [4–13] performance characteristics of this noteworthy technique of high recovery, low energy, simple modular design, and a flexibility choice of operational conditions. For reasons already specified elsewhere in this article, CCD units with single element modules should enable maximum volume reduction with minimum fouling effects, although modules with 2 or 3 elements each could also be used for such an application with somewhat lesser effectiveness. The preferred requirements to achieve maximum volume reduction by CCD should include feed of low pH (3–5), the adding an appropriate antiscalant, and the choosing of the appropriate conditions for the consecutive sequential batch process under fixed applied pressure conditions of declined flux. BWRO–CCD and BWRO–CCD–PFD operational trials under fixed pressure of declined flux conditions were already tried successfully [17]. The declined flux CCD operation could be optimized by the choosing one or several cross flow rates during the course of the sequential batch, an option not available with conventional RO techniques. If used for the exact same application as that of the batch SWRO unit [18] displayed in Fig. 12, a CCD unit of the same module configuration, operated under either fixed or variable pressure conditions, should

enable volume reduction without need of tanks for recycled concentrates and permeates with cross flow control optimized to yield maximum volume reduction during the course of the process with an enormous saving of energy compared with the very high energy requirements of the illustrated SWRO batch process [18] unit design displayed in Fig. 12.

6. Summary and concluding remarks

Single element (8´´) module(s) CCD units are characterized as being highly effective for small-scale production of permeates for diverse applications instead of convention RO techniques with many 4´´ or 2.5´´ diameter elements in staged or non- staged pressure vessels configurations. Apart from common applications, the said single element modules CCD units may be found useful for medical dialysis, volume reduction of difficult industrial effluents with high sulfate and silica contents as well as for the production of high quality permeates by a 2nd pass following a 1st pass in the same single element unit. The low energy and flexible operational modes of CCD apparatus with single element modules make them ideal for integration with clean renewable energy sources of variable power output such as derived from solar panels and/or wind turbines.

The extreme case study under review amplifies the enormous differences between the newly conceived CCD technologies and conventional RO methods since high recovery RO processes of low energy consumption without ERD are impossible by the latter.

Acknowledgements

Funds to *Desalitech Ltd*. by AQUAGRO FUND L.P. (Israel) and by Liberation Capital LLC (USA) are gratefully acknowledged.

References

[1] S. Loeb, S. Sourirajan, American chemical society advances in chemistry series, Am. Chem. Soc. 38 (1963) 117–132.
[2] N. Voutchkov, Membrane seawater desalination – overview and recent trends, IDA Conference, November 2–3, 2010, Huntington Beach, CA, USA.
[3] Status document "Desalination A National Perspective" sponsored by the National Research Council of the National Academies and published by the National Academies Press, Washington, DC, 2008. Available from: http://www.nap.edu/catalog/12184.html.
[4] A. Efraty, R.N. Barak, Z. Gal, Closed circuit desalination—A new low energy high recovery technology without energy recovery, Desalin. Water Treat. 31 (2011) 95–101.
[5] A. Efraty, R.N. Barak, Z. Gal, Closed circuit desalination series no-2: New affordable technology for sea water desalination of low energy and high flux using short modules without need of energy recovery, Desalin. Water Treat. 42 (2012) 189–196.
[6] A. Efraty, Closed circuit desalination series no-3: High recovery low energy desalination of brackish water by a new two-mode consecutive sequential method, Desalin. Water Treat. 42 (2012) 256–261.
[7] A. Efraty, Closed circuit desalination series no-4: High recovery low energy desalination of brackish water by a new single stage method without any loss of brine energy, Desalin. Water Treat. 42 (2012) 262–268.
[8] A. Efraty, J. Septon, Closed circuit desalination series no-5: High recovery, reduced fouling and low energy nitrate decontamination by a cost-effective BWRO-CCD method, Desalin. Water Treat. 49 (2012) 384–389.
[9] A. Efraty, Closed circuit desalination series no-6: Conventional RO compared with the conceptually different new closed circuit desalination technology, Desalin. Water Treat. 41 (2012) 279–295.
[10] A. Efraty, Z. Gal, Closed circuit desalination series No 7: Retrofit design for improved performance of conventional BWRO system, Desalin. Water Treat. 41 (2012) 301–307.
[11] R.L. Stover, N. Efraty, Low-energy consumption with closed-circuit desalination, Desalin. Water Reuse 43 (2012) 12–19.
[12] R.L. Stover, Industrial and brackish water treatment with closed circuit desalination reverse osmosis, Desalin. Water Treat. 51 (2013) 1124–1130.
[13] A. Efraty, Closed circuit desalination series no-8: Record saving of RO energy by SWRO-CCD without need of energy recovery, Desalin. Water Treat. 52(31–33) (2014) 5717–5730.
[14] Dow Liquid Separation, FILMTEC^{TM} Reverse Osmosis Membranes, Technical Manual, 2011. Available from: http://msdssearch.dow.com.asanexample.
[15] Specifications of the SWC6-MAX membrane element by Hydranautics, Available from: http://www.membranes.com/docs/8inch/SWC6MAX.pdf.
[16] Specifications of the ESPA2-MAX membrane element by Hydranautics. Available from: http://www.membranes.com/docs/8inch/ESPA2%20MAX.pdf.
[17] Undisclosed data of Desalitech Ltd.
[18] A.J. Tarquin, Sea water reverse osmosis systems to reduce concentrate volume prior to disposal, US Patent Application, Pub. No: US 2011/0036775 A1.